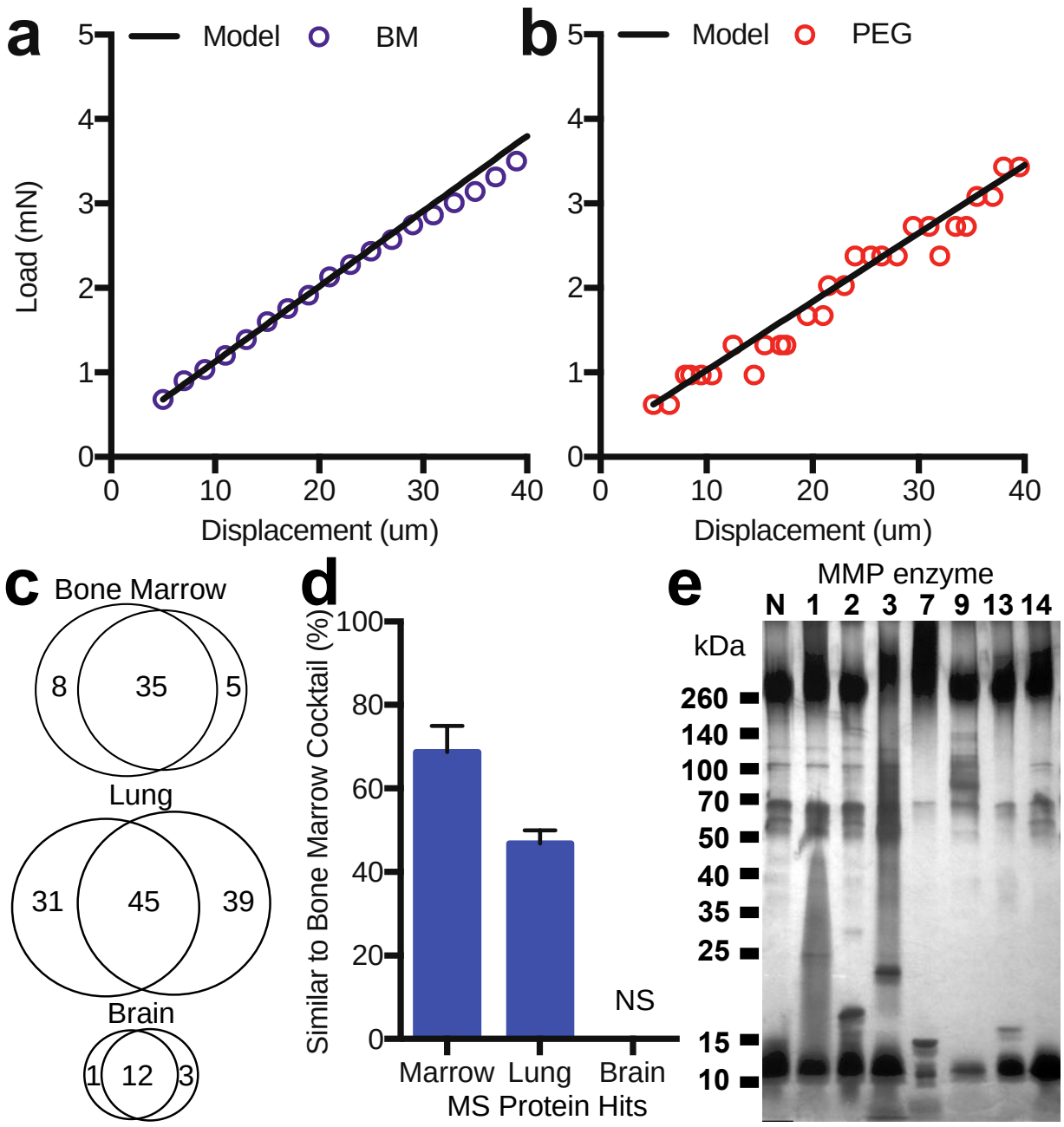


**Supplemental Figure 1. Validating algorithm using real tissue.** a) Representative compressive loading data from porcine bone marrow (Jansen et al., 2015) and b) the PEG bone marrow hydrogel matched to a Hertzian model for the calculated modulus (black line). c) Venn diagrams depicting protein hits from two different healthy human donors of bone marrow, lung, and brain tissues analyzed by LC-MS. d) The percentage of similarity the proteins found in LC-MS are to the bone marrow peptide cocktail identified using histology data from the Protein Atlas (NS=no similarity). e) Silver stain of human bone marrow ECM in the absence (N) or presence of active MMP enzymes.

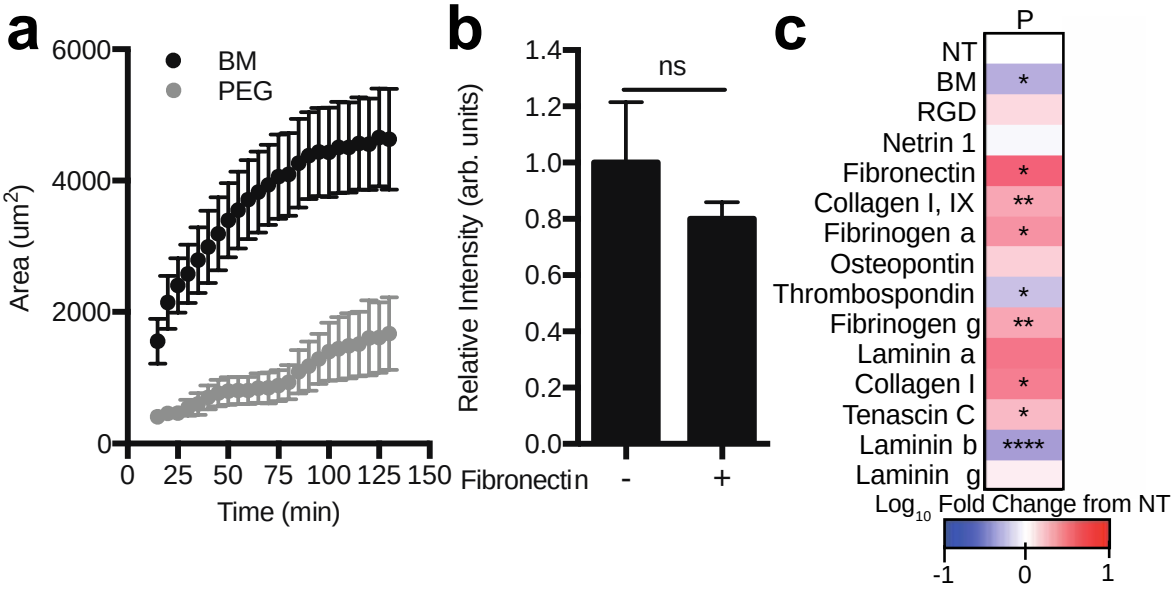


**Supplemental Figure 2. MSCs and breast cancer cells adhesion to bone marrow peptide cocktail.** a) MSC area over 2 hours for cells seeded onto a surface coupled with the bone marrow peptide cocktail (BM, same data as seen in Figure 2a) or PEG. b) Relative intensity of fluorescently tagged fibronectin passively adhered for 2 hours before imaging onto bone marrow peptide functionalized coverslips. c) Heat map depicting the $\log_{10}$ fold change in breast cancer cell area as a function of peptide treatment at 2 hours compared to no treatment (NT) for parental MDA-MB-231 cells (P) (BM=bone marrow peptide cocktail). Significance is determined using a two-tailed t-test where p=0.05 (N≥2, n≥20).

**Supplemental Video 1.** MSCs pre-treated with peptides seeded onto a coverslip coated with integrin-binding peptides.

**Supplemental Video 2.** MSCs seeded onto a coverslip coated with integrin-binding peptides.

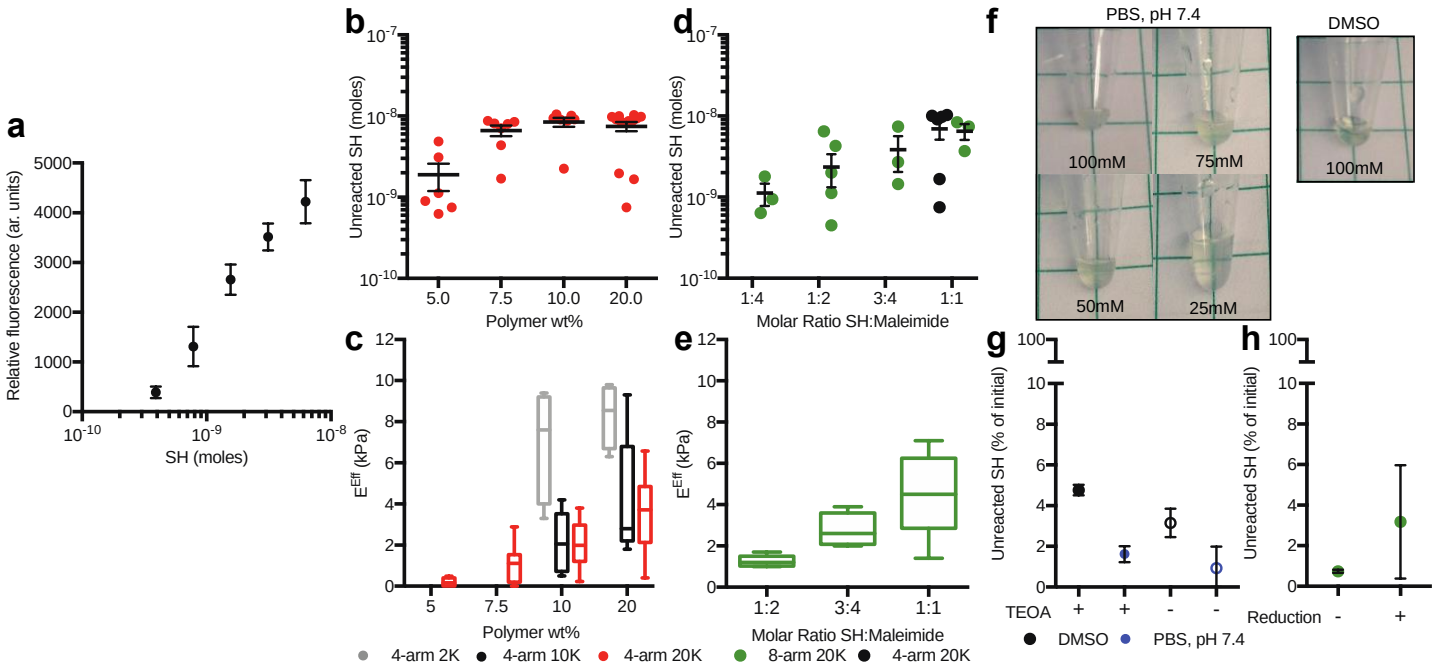


**Supplemental Figure 3. Modulating hydrogel properties to optimize bone marrow peptide cocktail incorporation.**

a) Relative fluorescence (494nm excitation, 517nm emission) correlates with moles of thiol (SH) using the MeasureIT thiol assay. b) Unreacted moles of thiol versus polymer weight percentage (wt%) for a 4-arm, 20K PEG (red). c) The effective Young's Modulus ($E^{Eff}$) for hydrogels made with 4-arm PEG at 2K, 10K, and 20K. d) Unreacted moles of thiols compared to the molar ratio of thiol to maleimide reactive groups for an 8-arm, 20K PEG and 4-arm, 20K PEG and the e) $E^{Eff}$ for the resulting 8-arm, 20K PEG hydrogels. f) Representative images showing peptide solubility in DMSO versus PBS at pH 7.4. Error bars represent the SEM (N≥2, n≥3 for mechanical testing; N≥1, n≥3 for unreacted thiol assay). g) The percentage of unreacted thiols when mono-functional peptides suspended in DMSO or PBS at pH 7.4 are added at a concentration of 1 mM to a solution of PEG dissolved in 2 mM TEOA or not in PBS at pH 7.4. h) The percentage of unreacted thiols after soaking reacted hydrogels in a reduction solution of sodium borohydride for 2 hours.

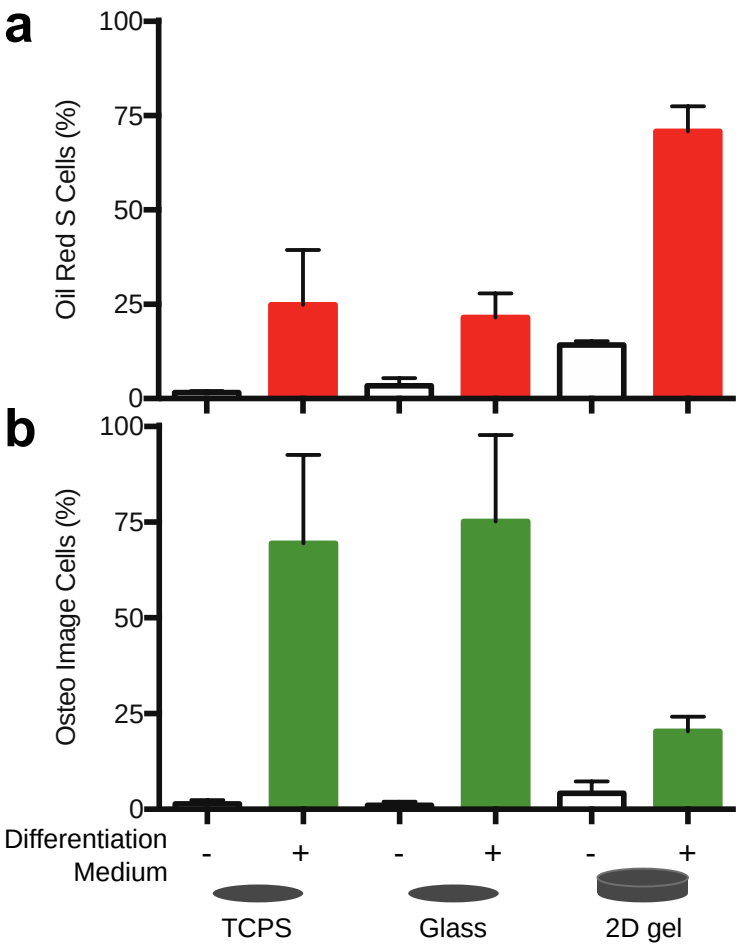


**Supplemental Figure 4. MSCs differentiation on multiple biomaterial platforms.** a) Fat differentiation quantified by Oil Red O and b) bone differentiation quantified by OsteoImage across different biomaterials: tissue culture polystyrene (TCPS) and a glass coverslip (glass) or 2D hydrogel at 4 kPa with the bone marrow peptides coupled to the surface. All platforms cells were exposed to fat, bone, or stem cell medium for 21 days before analysis. Error bars represent SEM (N=3, n=2).

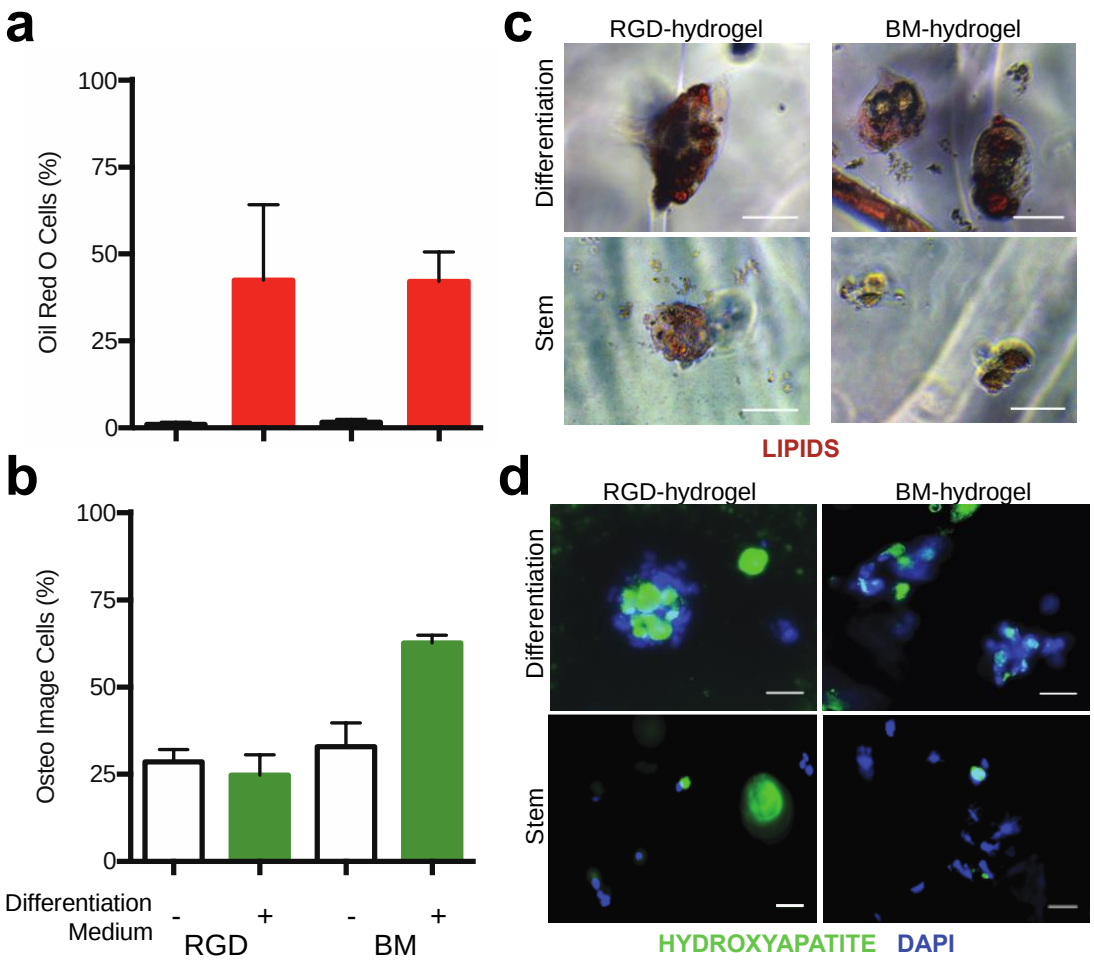


**Supplemental Figure 5. MSC differentiation in 3D hydrogels.** a) Fat differentiation quantified by Oil Red O and b) bone differentiation quantified by OsteoImage in a hydrogel with no degradability and 2 mM RGD (RGD) or the bone marrow hydrogel (BM). Representative images for MSCs stained with c) Oil Red O for lipids or d) OsteoImage for hydroxyapatite in both 3D platforms, scale = 50μm (N=3, n=2).

**Supplemental Table 1 References**


1 Knight, C. G. *et al.* The Collagen-binding A-domains of Integrins 1 1 and 2 1Recognize the Same Specific Amino Acid Sequence, GFOGER, in Native (Triple-helical) Collagens. *Journal of Biological Chemistry* **275**, 35-40, doi:10.1074/jbc.275.1.35 (2000).

2 Staatz, W. D. *et al.* Identification of a Tetrapeptide Recognition Sequence for the alpha2beta1 Integrin in Collagen. *The Journal of Biological Chemistry* **266**, 7363-7367 (1991).

3 Ruoslahti, E. RGD and other recognition sequences for integrins. *Annual Review of cell and developmental biology* **12**, 697-715 (1996).

4 Patterson, J. & Hubbell, J. A. Enhanced proteolytic degradation of molecularly engineered PEG hydrogels in response to MMP-1 and MMP-2. *Biomaterials* **31**, 7836-7845, doi:10.1016/j.biomaterials.2010.06.061 (2010).

5 Sternlicht, M. D. & Werb, Z. How matrix metalloproteinases regulate cell behavior. *Annu Rev Cell Dev Biol* **17**, 463-516, doi:10.1146/annurev.cellbio.17.1.463 (2001).

6 Uhlén, M. *et al.* Tissue-based map of the human proteome. *Science* **347**, 1260419 (2015).

7 Colognato, H. & Yurchenco, P. D. Form and function: The laminin family of heterotrimers. . *Developmental Dynamics* **218**, 213-234 (2000).

8 Zhang, W. M. *et al.* alpha 11beta 1 integrin recognizes the GFOGER sequence in interstitial collagens. *J Biol Chem* **278**, 7270-7277, doi:10.1074/jbc.M210313200 (2003).

9 Li, Z. The alphaMbeta2 integrin and its role in neutrophil function. *Cell Research* **9**, 171-178 (1999).

10 Bax, D. V., Rodgers, U. R., Bilek, M. M. & Weiss, A. S. Cell adhesion to tropoelastin is mediated via the C-terminal GRKRK motif and integrin alphaVbeta3. *J Biol Chem* **284**, 28616-28623, doi:10.1074/jbc.M109.017525 (2009).

11 Sakamoto, H. *et al.* Cell-type specific recognition of RGD- and non-RGD-containing cell binding domains in fibrillin-1. *Journal of Biological Chemistry* **271**, 4916-4922 (1996).

12 Yamada, K. M. Adhesive Recognition Sequence. *The Journal of Biological Chemistry* **266**, 12809-12812 (1991).

13 Humphries, J. D., Byron, A. & Humphries, M. J. Integrin ligands at a glance. *J Cell Sci* **119**, 3901-3903, doi:10.1242/jcs.03098 (2006).

14 Plow, E. F., Haas, T. A., Zhang, L., Loftus, J. & Smith, J. W. Ligand binding to integrins. *J Biol Chem* **275**, 21785-21788, doi:10.1074/jbc.R000003200 (2000).

15 Lishko, V. K. *et al.* Multiple binding sites in fibrinogen for integrin alphaMbeta2 (Mac-1). *J Biol Chem* **279**, 44897-44906, doi:10.1074/jbc.M408012200 (2004).

16 Yebra, M. *et al.* Recognition of the neural chemoattractant Netrin-1 by integrins alpha6beta4 and alpha3beta1 regulates epithelial cell adhesion and migration. *Developmental Cell* **5**, 695-707 (2003).

17 Prater, C. A., Plotkin, J., Jaye, D. & Frazier, W. A. The properdin-like type I repeats of human thrombospondin contain a cell attachment site. *Journal of Cell Biology* **112**, 1031-1040 (1991).

18 Barczyk, M., Carracedo, S. & Gullberg, D. Integrins. *Cell Tissue Res* **339**, 269-280, doi:10.1007/s00441-009-0834-6 (2010).

19 Camper, L., Hellman, U. & Lundgren-Åkerlund, E. Isolation, cloning, and sequence analysis of the integrin subunit α10, a β1-associated collagen binding integrin expressed on chondrocytes. *The Journal of Biological Chemistry* **273**, 20383-20389 (1998).

20 Tulla, M. *et al.* Selective binding of collagen subtypes by integrin alpha 1I, alpha 2I, and alpha 10I domains. *The Journal of Biological Chemistry* **276**, 48206-48212 (2001).

21 Marshall, J. F. *et al.* Alpha v beta 1 is a receptor for vitronectin and fibrinogen, and acts with alpha 5 beta 1 to mediate spreading on fibronectin. *Journal of Cell Science* **108**, 1227-1238 (1995).

22 Katoh, D. *et al.* Binding of alphavbeta1 and alphavbeta6 integrins to tenascin-C induces epithelial-mesenchymal transition-like change of breast cancer cells. *Oncogenesis* **2**, e65, doi:10.1038/oncsis.2013.27 (2013).

23 Wu, C., Chung, A. E. & McDonald, J. A. A novel role for alpha 3 beta 1 integrins in extracellular matrix assembly. *Journal of Cell Science* **108**, 2511-2523 (1995).

24 Dulabon, L. *et al.* Reelin Binds α3β1 Integrin and Inhibits Neuronal Migration. *Neuron* **27**, 33-44 (2000).